JOURNAL OF NEUROTRAUMA 28:579–594 (April 2011)

DOI: 10.1089/neu.2010.1626

Transplantation of Human Glial Restricted Progenitors and Derived Astrocytes into a Contusion Model of Spinal Cord Injury

Ying Jin,[1] Birgit Neuhuber,[1] Anita Singh,[1] Julien Bouyer,[1] Angelo Lepore,[2] Joseph Bonner,[1] Tim Himes,[1] James T. Campanelli,[3] and Itzhak Fischer[1]

Abstract

Transplantation of neural progenitors remains a promising therapeutic approach to spinal cord injury (SCI), but the anatomical and functional evaluation of their effects is complex, particularly when using human cells. We investigated the outcome of transplanting human glial-restricted progenitors (hGRP) and astrocytes derived from hGRP (hGDA) in spinal cord contusion with respect to cell fate and host response using athymic rats to circumvent xenograft immune issues. Nine days after injury hGRP, hGDA, or medium were injected into the lesion center and rostral and caudal to the lesion, followed by behavioral testing for 8 weeks. Both hGRP and hGDA showed robust graft survival and extensive migration. The total number of cells increased 3.5-fold for hGRP, and twofold for hGDA, indicating graft expansion, but few proliferating cells remained by 8 weeks. Grafted cells differentiated into glia, predominantly astrocytes, and few remained at progenitor state. About 80% of grafted cells around the injury were glial fibrillary acidic protein (GFAP)-positive, gradually decreasing to 40–50% at a distance of 6 mm. Conversely, there were few graft-derived oligodendrocytes at the lesion, but their numbers increased away from the injury to 30–40%. Both cell grafts reduced cyst and scar formation at the injury site compared to controls. Microglia/macrophages were present at and around the lesion area, and axons grew along the spared tissue with no differences among groups. There were no significant improvements in motor function recovery as measured by the Basso, Beattie, and Bresnahan (BBB) scale and grid tests in all experimental groups. Cystometry revealed that hGRP grafts attenuated hyperactive bladder reflexes. Importantly, there was no increased sensory or tactile sensitivity associated with pain, and the hGDA group showed sensory function returning to normal. Although the improved lesion environment was not sufficient for robust functional recovery, the permissive properties and lack of sensory hypersensitivity indicate that human GRP and astrocytes remain promising candidates for therapy after SCI.

Key words: axon growth; bladder control; motor and sensory function; neural stem cells; scar formation

Introduction

Spinal cord injury (SCI) results in functional deficits due to the disruption of ascending sensory and descending motor tracts. Autonomic dysfunction and neuropathic pain often accompany SCI and contribute to poor quality of patient life. Cell transplantation is a promising therapeutic strategy for SCI treatment to replace lost cells, improve the hostile environment of the lesion site, and provide a matrix for axon growth. Transplants of Schwann cells (Guest et al., 1997; Xu et al., 1995), olfactory ensheathing cells (Ramon-Cueto et al., 1998; Raisman and Li, 2007), fibroblasts modified to secrete trophic factors (Jin et al., 2002; Liu et al., 1999), bone marrow stromal cells (Himes et al., 2006), and neural stem cells (Lepore et al., 2006; McDonald et al., 1999) have shown to improve functional outcome in models of SCI.

While many studies have utilized various types of neural progenitors in models of SCI, only a few have addressed the therapeutic potential of glial progenitors, particularly with human cells. Glial-restricted progenitors (GRP) are the earliest progenitor cell type with a tripotential phenotype for cells derived from the embryonic spinal cord that include

[1]Department of Neurobiology and Anatomy, Drexel University College of Medicine, Philadelphia, Pennsylvania.
[2]Department of Neuroscience, Thomas Jefferson Medical College, Philadelphia, Pennsylvenia.
[3]Q Therapeutics, Inc., Salt Lake City, Utah.

oligodendrocytes and two types of astrocytes (Hill et al., 2004; Rao et al., 1998). GRP can be purified by cell sorting based on the A2B5 surface antigen and then expanded, as they retain an extensive ability for self-renewal (Rao et al., 1998). Rat GRP grafted into the intact spinal cord survived well, differentiated into glial phenotypes, and migrated along white matter tracts (Han et al., 2004). Acute transplants of rat GRP in a spinal cord contusion injury showed that GRP survived at the lesion site and differentiated into astrocytes and oligodendrocytes. Transplanted GRP also provided neuroprotection, and reduced the glial scar and the expression of inhibitory proteoglycans (Hill et al., 2004; Nout et al., 2010). Combined neuronal and glial-restricted progenitors grafted into contused spinal cord improved bladder and motor function and decreased thermal hypersensitivity (Mitsui et al., 2005). Similarly, grafting GRP modified to express neurotrophins resulted in improved function (Cao et al., 2005). Other studies utilized bone morphogenic proteins (BMP) to generate astrocytes from GRP (GDA), which provided a supportive environment that promoted regeneration and function in a hemisection injury model (Davies et al., 2006). However, there are no corresponding studies of either human GRP or GDA, which will ultimately be required for human clinical application.

In this study, we used human glial-restricted progenitor cells (hGRP) and astrocytes derived from hGRP (hGDA) to comprehensively study their anatomical and functional properties including cell survival, migration, and differentiation, as well as their effects on recovery of motor, sensory, and autonomic function following transplantation in a contusion injury. Similarly to previous studies with other types of human neural stem cells that used nude mice and rats (Hooshmand et al., 2009; Yan et al., 2007), we used immunodeficient NOD-scid (athymic) rats to avoid the extensive immune suppression typically required for long-term cellular engraftment. The hGRP and hGDA grafts showed excellent survival, glial differentiation, and extensive migration, with improvement of the lesion environment and no increase in sensory or tactile sensitivity associated with pain. However, with few exceptions there was no significant functional recovery, which is likely to require optimized administration and dosing parameters or additional interventions.

Methods

Animals

Female athymic rats (NTac:NIH-*Whn*) were obtained from Taconic Farms (Germantown, NY). They were housed 3 per cage with an air filter in an environmentally-controlled facility with a 12-h/12-h light/dark cycle. Food and water were available *ad libitum.* All procedures were approved by the Institutional Animal Care and Use Committee of Drexel University College of Medicine, and were carried out according to the National Institutes of Health (NIH) Guide for the Care and Use of Laboratory Animals.

Preparation of human glial-restricted progenitors

Human GRP were isolated from fetal cadaver brain tissue of gestational age 18–24 weeks. Tissue was procured by procurement specialists employed by Advanced Bioscience Resources (ABR; Alameda CA; FEIN 3005208435) following donor ID and informed consent SOPs and donor medical record review procedures. The tissue was manually and enzymatically dissociated to yield a single-cell suspension containing GRP, as well as other progenitors, microglia, red blood cells, endothelial cells, astrocytes, and neurons. The single-cell suspension was subjected to immunomagnetic purification using Miltenyi Biotec superparamagnetic bead technology, mouse monoclonal A2B5 antibody (an IgM antibody that recognizes c-series gangliosides on the cell surface of hGRP; Dubois et al., 1990; Saito et al., 2001), and microbead-conjugated anti-mouse antibody. Labeled cells were separated from unlabeled cells by passage through a magnetic field as previously described (Sandrock et al., 2010). Positively selected cells were cultured for 20 days (3 passages) in DMEM/F12 with N1 supplement and bFGF, harvested with TrypLE (Invitrogen, Carlsbad. CA), cryopreserved in Pro-Freeze/15% DMSO, and stored in vapor phase liquid nitrogen. The cells were characterized using a panel of antibodies representing antigens expressed by hGRP as follows: A2B5, $82.8 \pm 7.8\%$; PDGFRa, $91.5 \pm 6.6\%$; nestin, $86.9 \pm 6.1\%$; and GFAP, $70.3 \pm 11.6\%$ for hGRP. PSA-NCAM (neural progenitors and neurons), CD68 (microglia), and PECAM (endothelial cells) were expressed at low levels (Sandrock et al., 2010).

Preparation of GRP-derived astrocytes

Human GDA were prepared by treating hGRP with BMP-4 for 5 days before transplantation (Davies et al., 2006). Briefly, cells were plated at 1.5×10^6cell/cm^2 on poly-L-lysine coated 75 cm^2 flasks and poly-L-lysine coated cover-slips. After 24 h, hGRP culture medium (DMEM/F12, BSA, Pen/Strep, N2, with bFGF, 20 ng/mL; NT-3, 5 ng/mL; PDGF-AA, 10 ng/mL) was removed and replaced by basal medium with 50 ng/mL BMP-4 for 5 days. The cells on the flasks were harvested using 0.05% trypsin, washed, and resuspended at 4.9×10^4 cells/μL in HBSS for transplantation. Additional cells on cover-slips were immunostained with antibodies against A2B5 and GFAP to confirm cell differentiation.

Surgical procedure

A total of 51 athymic rats (age = 12 weeks) were used in this study. Forty-seven athymic rats received a contusion lesion and were randomly divided into three groups receiving transplants of hGRP (n = 22), hGDA (n = 8), or HBSS medium (control, n = 14) 9 days after injury (3 rats did not survive the lesion surgery). Three hGRP-transplanted rats were excluded for early examination of cell survival (n = 2), or due to sickness (n = 1). Four uninjured athymic rats were used as sham controls (sham, n = 4) for cystometry.

After anesthesia with XAK, a mixture containing xylazine (10 mg/mL), acepromazine maleate (0.7 mg/kg), and ketamine (95 mg/kg) injected IP (n = 24), a laminectomy was performed at T10, and a contusion lesion was made with the Multicenter Animal Spinal Cord Injury Study (MASCIS) impactor (10-g weight dropped 25 mm). Muscle and skin were closed in layers. Because 3 animals died during surgery with XAK anesthesia, we used isoflurane to anesthetize the remaining animals (n = 23).

Nine days after contusion, the animals were re-anesthetized with isoflurane for transplantation of control medium or cells. Human GRP were thawed and counted. After washing with culture medium, the cells were resuspended at 1×10^5

cells/μL in HBSS without Ca^{++}/Mg^{++} and kept on ice for transplantation. Human GDA were prepared by treating hGRP with BMP-4 5 days before transplantation. Cells were collected as described above. The animals were placed in a spinal stereotaxic frame, and the lesioned spinal cord was exposed. Using a 10 μL Nanofil syringe (World Precision Instruments, Sarasota, FL) with a 33-gauge needle, HBSS (10 μL) or cells (10 μL, 1×10^5cells/μL) were injected into the spinal cord. Five microliters of HBSS or cells suspended in HBSS were injected at the lesion center, and 2.5 μL were injected 2 mm rostral and caudal to the lesion center. Using a Kite manual micromanipulator (World Precision Instruments), the needle was set at the lesion center along the midline and inserted into the spinal cord 1.5 mm from the dura. The needle was removed from the first injection site and moved on the midline 2 mm rostrally and caudally using the scale on the micromanipulator, and inserted into the cord 1.5 mm deep from the dura. Cells or HBSS was injected at 20 nL/sec using a nanoliter pump controller (World Precision Instruments). After 1 min the tip was slowly withdrawn. To prevent blockage, the syringe was thoroughly flushed with HBSS between injections. The rats were placed back in their cages with heating pads, and closely observed until awake. Saline was injected subcutaneously immediately after lesion and transplantation, and was also injected daily for 7 days. Ampicillin (Bristol-Myers Squibb, Princeton, NJ) was injected daily for 7 days postoperatively. The bladders were manually expressed twice a day for 3 weeks, and then once a day until sacrifice.

Evaluation of motor and sensory function

Open-field locomotion. The rats were placed in an enclosure and scored by two blinded observers according to the Basso, Beattie, and Bresnahan (BBB) rating scale (Basso et al., 1995) before contusion, 2–3 days after contusion, and once a week after transplantation for 8 weeks. Inter-rater reliability was 95%.

CatWalk gait analysis. Using the CatWalk program, paw prints were labeled and the following gait parameters were measured and compared: (1) regularity index, which grades the degree of interlimb coordination; (2) base of support, which measures the distance between either the front or hindlimbs; (3) stride length, which measures the length of a stride during locomotion; (4) swing duration, which measures the time between swing phases for each limb; and (5) phase dispersion, which is a more quantitative measure of interlimb coordination. CatWalk analysis was performed every week on animals with a BBB score above 10.

Grid test. The rats walked on an elevated grid (36 cm L $\times$ 38 cm W $\times$ 30 cm H with 1.2 $\times$ 1.2-cm openings) for 2 min. The total number of good steps over the total number of steps were counted for each hindpaw. Grid tests were performed weekly on animals with a BBB score above 10.

Thermal sensitivity test. This test measures the latency of limb withdrawal in response to a heat stimulus applied to the paw. The animals were placed on a platform and a movable radiant heat source (25–29°C) was applied to a forepaw. If the paw was not withdrawn within 30 sec the heat source was removed to prevent tissue damage. Five trials were run for each paw with a 15-min interval between each trial to prevent sensitization. The withdrawal latency was measured for the last four trials and averaged (Cao et al., 2008). Heat testing was performed weekly on animals with a BBB score of 10 or above.

Mechanical sensitivity test. To determine the degree of tactile sensory changes present after SCI, Von Frey hair monofilaments (VFH; Stoelting Co., Wood Dale, IL) were applied to the plantar surface of the hindpaw using a modified version of the up-down method (Chaplan et al., 1994). To ensure that all rats could withdraw their hindpaws from an unpleasant stimulus, plantar VFH was not initiated unless hindlimb weight support recovered according to BBB testing (BBB score 10 or above). The rats were placed in an inverted acrylic glass cage (20.25 $\times$ 13.5 $\times$ 15.25 cm) with a wire mesh bottom (0.635 cm grid size) allowing access to the plantar surface of the hindpaws. Testing commenced with the 15.14-g VFH filament applied perpendicularly at a consistent rate ($\sim$1 sec) to the plantar surface of the hindpaw (1 cm posterior to the foot pads). When a brisk, immediate paw withdrawal occurred, the next lower VFH was applied. When no hindpaw withdrawal occurred, the next higher VFH was applied. Ten VFH applications were used, and approximately 30–60 sec separated each touch. If an animal lifted the paw, the trial was discarded and the animal was retested following the standard interstimulus interval. The tactile sensory threshold was defined as the lowest gram force needed to produce hindpaw withdrawal on at least 50% of its applications. The animals were tested before surgery and before sacrifice at 8 weeks.

Evaluation of bladder function

Urine chemstrips. Daily records of bladder size (large, moderate, or small), and urine color (clear, cloudy, or bloody) were obtained. In addition, Chemstrips (Chemstrip9; Roche Diagnostics Corp., Indianapolis, IN) were used 2–3 days after injury and once a week after transplantation until sacrifice to examine pH, leukocytes, protein, blood, and hemoglobin in the urine.

Awake cystometry. Eight weeks after transplantation, the rats were anesthetized using isoflurane, and a catheter was implanted in the bladder (Mitsui et al., 2003, 2005). Briefly, the bladder was exposed by a midline lower abdominal incision, and a polyethylene catheter (PE-60; Clay Adams, Parsippany, NJ) was implanted into the bladder through the dome. The bladder catheter was tunneled subcutaneously and exited through the skin on the back, as previously described (Mitsui et al., 2003). The rats were then placed in a restraining cage (KN-326; Natsume, Tokyo, Japan) and allowed to recover for 1–2 h. The bladder catheter was connected to a pressure transducer (World Precision Instruments), and a microinjection pump (STC-523; Terumo, Tokyo, Japan). Room-temperature saline was infused at a rate of 0.1 mL/min, and intravesical pressure was recorded to compare urodynamic parameters in each group. The maximal voiding pressure, post-void residual urine (obtained by emptying the bladder at the end of the last recorded micturition using a syringe attached to the catheter that was inserted in the bladder), bladder capacity (urine volume/void + residual urine), and the frequency of

detrusor hyperreflexia (DHR) per micturition episode (peaks above 2 SD of the baseline recording) were compared in each group.

Tissue preparation

Animals were anesthetized with IP injections of sodium pentobarbital (100 mg/kg; Abbott Laboratories, North Chicago, IL), and transcardially perfused with 200 mL saline, followed by 500 mL of ice-cold 4% paraformaldehyde fixative in phosphate buffer (PB; pH 7.4). Several segments of spinal cord were collected: (1) a segment containing the lesion area and extending 5 mm rostral and caudal to the lesion/transplant, (2) rostral and caudal segments adjacent to the lesion-containing segment, and (3) lumbo-sacral spinal cord segments. The bladder was also collected and the weight and size were measured. Tissues were post-fixed in the same fixative for 3 days, and then transferred to a solution of 30% sucrose in 0.1 M PB for 5 days. Spinal cord segments were embedded in M1 (Fisher Scientific, Pittsburgh, PA), and the lesion-containing segment and segments rostral and caudal to it were cut into 20-μm sagittal sections on a cryostat, and mounted onto gelatin-coated slides in six serial sets. The lumbo-sacral spinal cord segments were cut into 30-μm cross sections and immunostained free-floating.

Immunocytochemistry (injury/transplant area)

Sagittally cut spinal cord sections were processed for Nissl myelin staining, and immunocytochemistry with antibodies against human nuclei (HuNA) to identify hGRP and hGDA, GFAP for astrocytes, Olig2 as a general marker for the oligodendrocyte lineage, NG2 for glial scar formation, Iba-1 for macrophage/microglia, SMI-31R for neurofilament to identify general axon growth, serotonin (5-HT) for descending serotonergic axons, and calcitonin gene-related peptide (CGRP) for ascending sensory axons (for antibody dilutions and sources see Table 1). Spinal cord sections were washed four times in PBS and blocked in 10% goat serum for 1 h. Primary antibodies were incubated with 10% goat serum in PBS containing 0.3% Triton X-100 at room temperature overnight. Species-specific secondary antibodies (goat anti-mouse or anti-rabbit conjugated to FITC or rhodamine, 1:400; Jackson ImmunoResearch, West Grove, PA) were applied for 2 h at room temperature, and the slides were cover-slipped with Vectashield (Vector Laboratories, Burlingame, CA) containing the nuclear counterstain 4′,6′-diamidino-2-phenylindole (DAPI). Fluorescently stained slides were stored at 4°C.

Immunocytochemistry (lumbar area)

Cross-sectioned lumbo-sacral tissues (L6–S1) were immunostained free-floating (Mitsui et al., 2005), with antibodies against 5-HT, CGRP, GAP-43, and vanilloid receptor type 1 (VR-1; (Table 1). Every 10th section across all groups was stained for each antibody. The sections were blocked with 10% goat serum in PBS for 2 h, and then incubated with the appropriate primary antibodies and 2% goat serum in PBS containing 0.3% Triton X-100 at 4°C for 24–72 h, and reacted with a species-specific biotinylated secondary antibody and ABC reagent (Vector Laboratories), each for 2 h at room temperature. Staining was visualized with Sigma fast DAB (Sigma-Aldrich, St. Louis, MO). The sections were mounted on gelatin-coated slides, dehydrated in graded ethanol, cleaned, and cover-slipped.

Quantitative analysis of cell numbers

Quantification of transplant survival and migration. HuNA was used to selectively identify transplant-derived cells of human origin at 8 weeks post-transplantation ($n = 3$ animals/group). Images of $HuNA^+$ immunofluorescence from the entire extent of a 12-mm segment of sagittally-sectioned spinal cord centered about the lesion epicenter were obtained with a Zeiss Imager.Z1 microscope at 20× magnification using a Zeiss AxioCam HRc camera. The images were then digitally "stitched" together with Zeiss AxioVision software. Total numbers of $HuNA^+/DAPI^+$ cells were manually counted in every sixth section throughout the stitched image. The spinal cord was subdivided in the rostral-caudal axis into 1-mm blocks centered about the lesion epicenter. Total numbers of $HuNA^+$ cells within each 1-mm block were counted,

Table 1. List of Antibodies Used for Immunohistochemical Staining

Antibody	*Host*	*Dilution*	*Manufacturer*	*Specificity*
Sagittal sections				
Human nuclei	Mouse	1:200	Chemicon	Human nuclei
GFAP	Rabbit	1:2000	Chemicon	Astrocytes
NG2	Rabbit	1:250	Chemicon	CSPG (NG2) deposition
SMI-31R	Rabbit	1:1000	Covance	General fiber growth
5-HT	Rabbit	1:20,000	Immunostar	Serotonergic fibers
CGRP	Rabbit	1:2000	Peninsula	Sensory fibers
Ki67	Rabbit	1:1000	Chemicon	Cell proliferation
Olig2	Rabbit	1:500	Chemicon	Oligodendrocytes
Cross sections				
CGRP	Rabbit	1:2000	Peninsula	Sensory fibers
5-HT	Rabbit	1:20,000	Immunostar	Serotonergic fibers
GAP-43	Mouse	1:50,000	Chemicon	Axonal growth
VR-1	Guinea pig	1:5000	Chemicon	Unmyelinated C-fibers

GFAP, glial fibrillary acidic protein; 5-HT, serotonin; CGRP, calcitonin gene-related peptide; VR-1, vanilloid receptor type 1; CSPG, chondroitin sulfate proteoglycan.

Chemicon International, Temecula, CA; Immunostar, Hudson, WI; Peninsula Laboratories, San Carlos, CA; Covance Inc., Princeton, NJ.

and total numbers of cells in each section were obtained by summing all 1-mm blocks. Cell numbers from all sections were summed and multiplied by 6 to obtain the total number of surviving cells in the entire spinal cord, as well as the total number of surviving cells at each successive 1-mm distance from the lesion epicenter. Values at each distance were also expressed as a percentage of the total number of surviving cells in the entire spinal cord.

Quantification of cell differentiation and proliferation. For astrocyte differentiation, $HuNA^+$ hGRP or hGDA that were double-labeled with the lineage-specific astrocyte marker GFAP were counted in sagittal sections at 8 weeks post-transplantation ($n = 3$ animals/group). Double-labeling was assessed in 1-mm blocks, as described above for $HuNA^+$ cell counts. The proportions of $HuNA^+/GFAP^+$ astrocytes were then expressed as a percentage of the total number of surviving $HuNA^+$ transplant-derived cells at the lesion epicenter, and at 2, 4, and 6 mm rostral or caudal to the epicenter. For oligodendrocyte differentiation, double staining of HuNA and Olig2 was counted in the transplant area, as well as the migration area (near the end of the section, about 6 mm from the transplant epicenter), in sagittal sections at 8 weeks post-transplantation (n = 3 animals/group). For cell proliferation, double staining of HuNA and Ki67 was counted using the same method as for oligodendrocytes. Double images of $HuNA^+$ cells and either Olig2 or Ki67 were taken using Slidebook at 20× magnification from 4 slides in both the transplant and migration areas. Total $HuNA^+$ cells and cells expressing $Olig2^+/HuNA^+$ or $Ki67^+/HuNA^+$ were counted and expressed as a percentage of total $HuNA^+$ transplant-derived oligodendrocytes or proliferating cells in the transplant and migration areas.

Measurement of spared tissue and cyst volume

Using Stereo Investigator, the volume of spared tissue and cyst were assessed in a blinded fashion in sagittal Nissl myelin stained sections. From each animal, every 30th cryostat section (600-μm intervals) was used to determine the total volume of a 13-mm-long segment centered at the contusion/transplantation epicenter, and the spared tissue within this segment. Tissue was considered spared if areas contained healthy-looking spinal neurons and myelin, and lacked cysts. Similarly, cyst volumes were determined within the lesion area. Using Stereo Investigator, spared tissue and cysts can be marked with different colors on each section. The system then calculates the total volume and provides the fraction of each part for each animal. Data were presented as percentages of total cord volume for spared tissue, and of lesion/transplant volume for cysts.

Quantitative analysis of glial scar

To examine if transplanted hGRP and hGDA modulated the lesion environment, the extent of astrocytes and proteoglycans were assessed with immunocytochemical staining of GFAP and NG2. Expression was evaluated following Hill's method (Hill et al., 2004). Briefly, the intensity of $GFAP^+$ and $NG2^+$ staining around the lesion at the center, as well as the rostral and caudal boundaries, was ranked on a five-point subjective intensity scale (5 = high intensity; 3 = medium intensity; 1 = low intensity).

Evaluation of changes in the lumbar spinal cord

Five sections of similar size, chosen at equal distances (every 10th section from L6–S1 was used for VR-1, CGRP, and 5-HT staining), were viewed with 10× (VR-1 and CGRP) and 20× (5-HT) objectives, and images were captured using a DC-330 CCD color video camera (DAGE-MTI, Inc., Michigan City, IN) attached to a Leica DMRBE microscope (Leica Microsystems; Bannockburn, IL). Images were converted using NIH ImageJ software into pixels according to a gray scale. In each image, the background level was determined from an area of ventral funiculus that did not exhibit immunoreactivity (IR). This background level was used to set the threshold between labeled pixels and background pixels. The illumination intensity was held constant through the analysis of the images from both the experimental operated and unoperated rats. A standard sized rectangle was overlaid on the dorsal horn (such that the top right corner of the rectangle was just below the exiting root in the dorsal horn), and the labeled area within the rectangle was measured, and is presented as area fraction (%).

Statistical analysis

A two-way analysis of variance (ANOVA) comparing control versus experimental groups over time, with time taken as a repeated measure, was used to analyze the behavioral data, with significance set at $p < 0.05$. *Post-hoc* analysis was performed using the Bonferroni test. One-way ANOVA was used for cyst volume and glial scar analysis, as well as changes in the lumbar spinal cord. Student's *t*-test was used for quantification of transplant survival, migration, differentiation, and proliferation.

Results

hGRP and hGDA survive, differentiate, and migrate extensively

Glial-restricted progenitors (hGRP) were prepared from fetal human brain tissue sorted by the A2B5 surface antigen. GRP-derived astrocytes (hGDA) were prepared from hGRP by treatment with BMP-4 for 5 days, which resulted in dramatic morphological differentiation into cells with multiple short processes. Athymic rats received moderate contusions at T10 and were transplanted 9 days after injury with control medium (HBSS), hGRP, or hGDA. By using athymic rats we avoided the need for immunosuppressive drugs, which are otherwise necessary for survival of human cell grafts. Eight weeks after transplantation, both hGRP and hGDA transplants showed excellent survival and extensive migration within the host tissue, as documented by immunostaining with human-specific nuclear antibodies HuNA (Fig. 1I and II). Quantitative analysis of grafted cells using HuNA indicated that the total number of cells increased over threefold for the hGRP graft, and twofold for the hGDA graft (Fig. 1IIIA), with significantly less expansion for the pre-differentiated hGDA relative to hGRP (3.46 ± 0.28 million cells for hGRP, and 2.03 ± 0.34 million cells for hGDA; $p = 0.031$ by *t*-test). There was, however, minimal indication of proliferation by 8 weeks, when the grafted cells were analyzed with the mitotic marker Ki67 (Fig. 2III). Transplanted cells were present throughout the lesion site and extensively migrated into the host tissue in both the rostral and caudal directions over a distance of

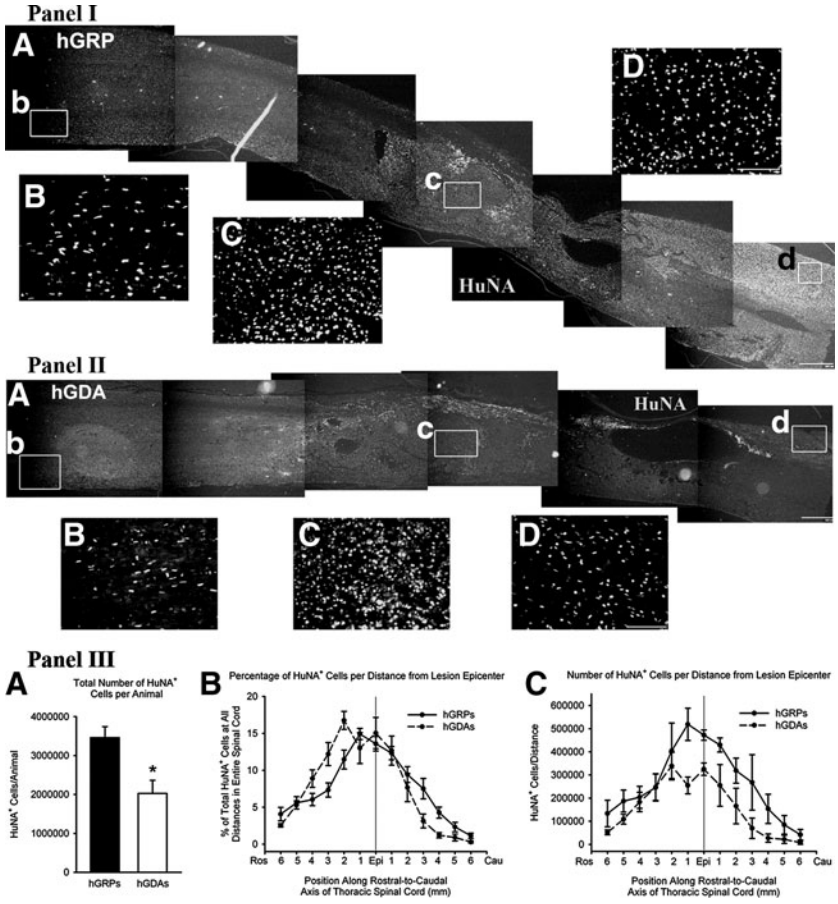

FIG. 1. Robust survival and migration of hGRP and hGDA. $HuNA^+$ hGRP and hGDA transplant-derived cells robustly survived and migrated in both rostral and caudal directions. Panels **I** (hGRP) and **II** (hGDA) show the distribution of transplanted cells in the entire section shown in **A** (scale bar = 500 μm), and high-magnification images from areas (marked by boxes b, c, and d) caudal to the injury (**B**), at the center of the transplant (**C**), and rostral to the injury (**D**; scale bar = 100μm). Panel **III** shows total numbers of $HuNA^+$ cells and distribution of $HuNA^+$ cells in the hGRP and hGDA groups. Following transplantation of 1.0×10^6 cells per animal, $3.46\times10^6\pm0.28$ total hGRP-derived cells survived in the entire spinal cord at 8 weeks post-transplantation, while $2.03\times10^6\pm0.34$ total hGDA-derived cells survived at this time point (**A**). $HuNA^+$ cells migrated in both rostral and caudal directions up to distances of at least 6 mm from the injection site, and the patterns of migration were similar for both the hGRP and hGDA groups (**B**). Even with this extensive migration, the vast majority of $HuNA^+$ cells were located within 2–3 mm rostral and caudal of the injection site, with a larger proportion of cells in the rostral direction in both transplant groups. When expressed as total numbers of cells, the migration plots show that significantly greater numbers of $HuNA^+$ cells survived in the hGRP group compared to the hGDA group, particularly close to the lesion epicenter and injection sites (**C**; hGRP, human glial-restricted progenitor; hGDA, astrocytes derived from hGRP; HuNA, antibodies against human nuclei; Ros, rostral; Cau, caudal; Epi, epicenter).

several segments. Interestingly, there was a slight bias in migration, with more cells migrating rostrally than caudally (Fig. 1IIIB and C). Close to the lesion, migrating cells were located in both gray and white matter, whereas further away from the lesion most migrating cells were found in the white matter.

Analysis of the phenotypic fate of cells showed that most of the hGRP and hGDA differentiated into glial cells with no undifferentiated cells (expressing nestin) detected at 8 weeks after transplantation (data not shown). Double staining with antibodies against human nuclei and GFAP indicated that the majority of hGRP and hGDA differentiated into astrocytes (Fig. 2IA). About 80% of the $HuNA^+$ cells around the lesion epicenter were also $GFAP^+$, which decreased to about 40–50% along the migration pathway at a distance of 6 mm (Fig. 2IB), with the hGDA graft showing an overall higher percentage of $GFAP^+$ cells ($61.3\pm3\%$ for hGRP and $70.7\pm3\%$ for hGDA; $p = 0.047$ by t-test). Again, there was a bias in the distribution of cells, with more $GFAP^+$ cells migrating rostrally than caudally. Double staining against human nuclei and Olig2 (Fig. 2IIA) indicated that few of the grafted cells differentiated into oligodendrocyte progenitors or oligodendrocytes at the lesion site (< 10%), though this number increased dramatically in the migration region (30–40%), with no significant differences between hGRP and hGDA (Fig. 2IIB). Double staining with antibodies against human nuclei and Ki67 (Fig. 2IIIA), a mitotic marker, showed that most hGRP and hGDA had ceased to proliferate, with about 3% of grafted cells labeled at the graft area, and about 6–7% at the migratory regions (Fig. 2IIIB). Again, there were no significant differences between hGRP and hGDA. Taken together, these results suggest that 8 weeks after transplantation, hGRP and

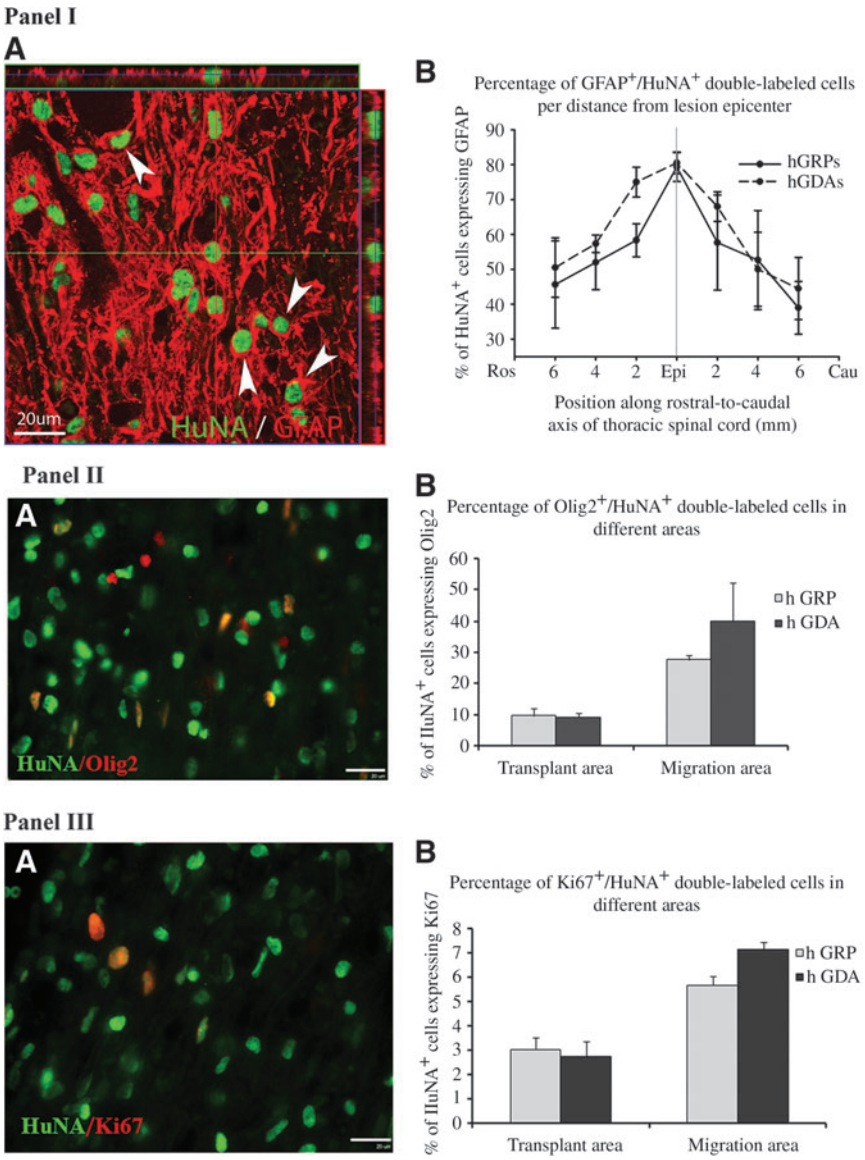

FIG. 2. Differentiation and proliferation of grafted cells. Transplanted HuNA$^+$ hGRP and hGDA differentiated into GFAP$^+$ astrocytes by 8 weeks post-transplantation. Panel **IA** represents a region in an hGRP-transplanted animal with migrating cells seen approximately 6 mm rostral to the injection site. About 80% of all HuNA$^+$ cells co-expressed the astrocyte marker GFAP at the injection sites (panel **IB**). This percentage decreased to 40–50% at greater distances from the injection sites. There was no significant difference between the two groups (scale bars = 20 μm). Transplanted HuNA$^+$ hGRP and hGDA also differentiated into Olig2$^+$ oligodendrocytes. Panel **IIA** represents a region in an hGRP-transplanted animal with migrating cells seen approximately 6 mm rostral to the injection site. Fewer HuNA$^+$ cells (< 10%) differentiated into Olig2$^+$ oligodendrocytes in the lesion area (panel **IIB**). More HuNA$^+$ cells (30–40%) differentiated into oligodendrocytes in the migration area (panel **IIB**). There was no significant difference in both areas between hGRP and hGDA. Double staining with HuNA and Ki67, a marker for cell proliferation, showed that few HuNA$^+$ cells proliferated in both the lesion (about 3%) and migration areas (6–7%) in the hGRP and hGDA groups (panels **IIIA** and **B**). There was also no difference between hGRP and hGDA (scale bars = 20 μm in panels **IIA** and **IIIA**; hGRP, human glial-restricted progenitor; hGDA, astrocytes derived from hGRP; HuNA, antibodies against human nuclei; GFAP, glial fibrillary acidic protein).

hGDA had differentiated into mature cell types with a similar pattern of phenotypic distribution.

hGRP and hGDA modulate the host environment

Nissl myelin staining showed that the contusion caused severe damage at the lesion site, including the formation of fluid-filled cavities (cysts), leaving little spared tissue as previously reported (Mitsui et al., 2005). In the transplant groups, hGRP and hGDA filled the lesion site with only a few cysts remaining at or near the host/graft interface. In contrast, control injury animals had large cysts embedded with host cells that had infiltrated the lesion area (Fig. 3A). Cyst and spared tissue volumes were measured using Stereo Investigator and calculated as percentages of total spinal cord volume at the lesion site. No significant differences were

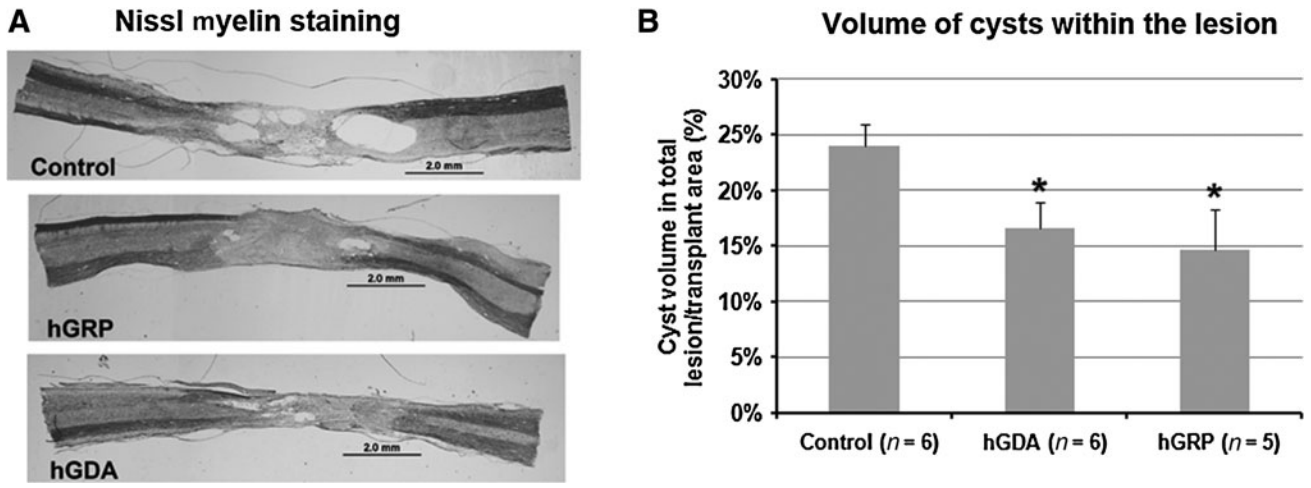

FIG. 3. Nissl myelin staining and cyst volumes. (**A**) Nissl myelin staining shows the lesion/transplant areas in the different experimental groups. In control animals, endogenous cells had incompletely infiltrated the lesion area, leaving many cysts within the lesion and at the interface between lesion and host. In animals transplanted with hGRP and hGDA, cells filled most of the lesion area, with fewer cysts within the lesion and at the host/graft interface (scale bars = 20 μm). (**B**) Cyst volumes in animals with cell transplants were smaller than in controls. The volume of cysts within the lesion area, measured in controls and transplanted animals, is presented as percentages of the entire lesion/transplant area. Cyst size was significantly reduced in both transplant groups relative to controls ($^*p < 0.05$). There was no significant difference between the hGRP and hGDA groups (hGRP, human glial-restricted progenitor; hGDA, astrocytes derived from hGRP).

observed in spared tissue volume among controls (77.0%), and the hGRP (70.3%) and hGDA (66.2%) groups. However, comparing the percentage of cyst volume within the lesion/transplant area showed that cyst volumes were smaller in hGRP- and hGDA-transplanted animals than in controls (Fig. 3B; $p < 0.05$). There was no significant difference between the hGRP and hGDA groups.

Accumulation of $GFAP^+$ astrocytes at the host/lesion interface in the control group (Fig. 4A) showed an outline of the lesion area; however, in hGRP- and hGDA-transplanted animals, there was no clear outline of the injury because of the abundance of transplanted cells and their contiguous presence in the host tissue (Fig. 4A). Intensity of $GFAP^+$ staining was significantly higher in the control group than in both the hGRP and hGDA groups in three measurement areas: the center and the rostral and caudal boundaries of the lesion/transplant (Fig. 4B). To analyze the presence of chondroitin sulfate proteoglycan (CSPG)-containing scar tissue around the injury we stained for NG2, a major component of CSPG. The analysis showed strong NG2 expression at the interface between the lesion and the host in the control group. In contrast, there was reduced staining in both hGRP- and hGDA-populated lesion areas, suggesting that these grafts reduce scar formation (Fig. 4C). Thus the staining of $NG2^+$ and $GFAP^+$ showed similar patterns of reduced levels in the hGRP and hGDA groups compared to the control group (Fig. 4D).

Macrophages and microglia extensively infiltrate lesion and transplants

In normal athymic rats, moderate numbers of macrophages and microglia were identified in the spinal cord stained with Iba-1 (data not shown). In contrast, in control injury animals there were high numbers of activated macrophages and microglia that infiltrated the lesion site 8 weeks after contusion lesion. In addition, activated macrophages and microglia were found in the surrounding tissue (Supplementary Fig. 1A; see online supplementary material at http://www.liebertonline.com). A similar distribution of macrophages and microglia was observed in the hGRP and hGDA groups, where macrophages and microglia were found among hGRP and hGDA in the transplant area (Supplementary Fig. 1B). Despite the large influx of activated macrophages and microglia, survival of transplanted cells was excellent.

Reduced scarring does not result in increased axon growth

To evaluate axon growth into the lesion/transplant area, we immunostained sections with the following: (1) antibodies against SMI-31R for neurofilaments (NF) to identify axon growth in general, (2) antibodies against 5-HT to identify descending serotonergic axons, and (3) antibodies against CGRP to identify ascending afferent axons. NF^+ axons were observed near the rostral and caudal edges of the lesion/transplant (Supplementary Fig. 2IA; see online supplementary material at http://www.liebertonline.com) in all groups, with no difference in their distribution. Some axons could be seen in the spared host tissue surrounding the lesions/transplants, and some were also present in the transplants or lesions. We did not find significant differences in axon growth in the hGRP- and hGDA-treated groups, even though they had reduced glial scarring and CSPG expression compared to controls. $CGRP^+$ axons were observed along the spared tissue surrounding the transplant/lesion in all groups (Supplementary Fig. 2II). Few $CGRP^+$ axons were found inside the transplants and lesions. Similarly, most 5-HT^+ axons stopped at the rostral edge of the host/graft or lesion interface (Supplementary Fig. 2III), and only a few entered into the lesion/transplant area as well as into the rim of spared tissue. Only a few 5-HT^+ axons were present in the cord below the lesion

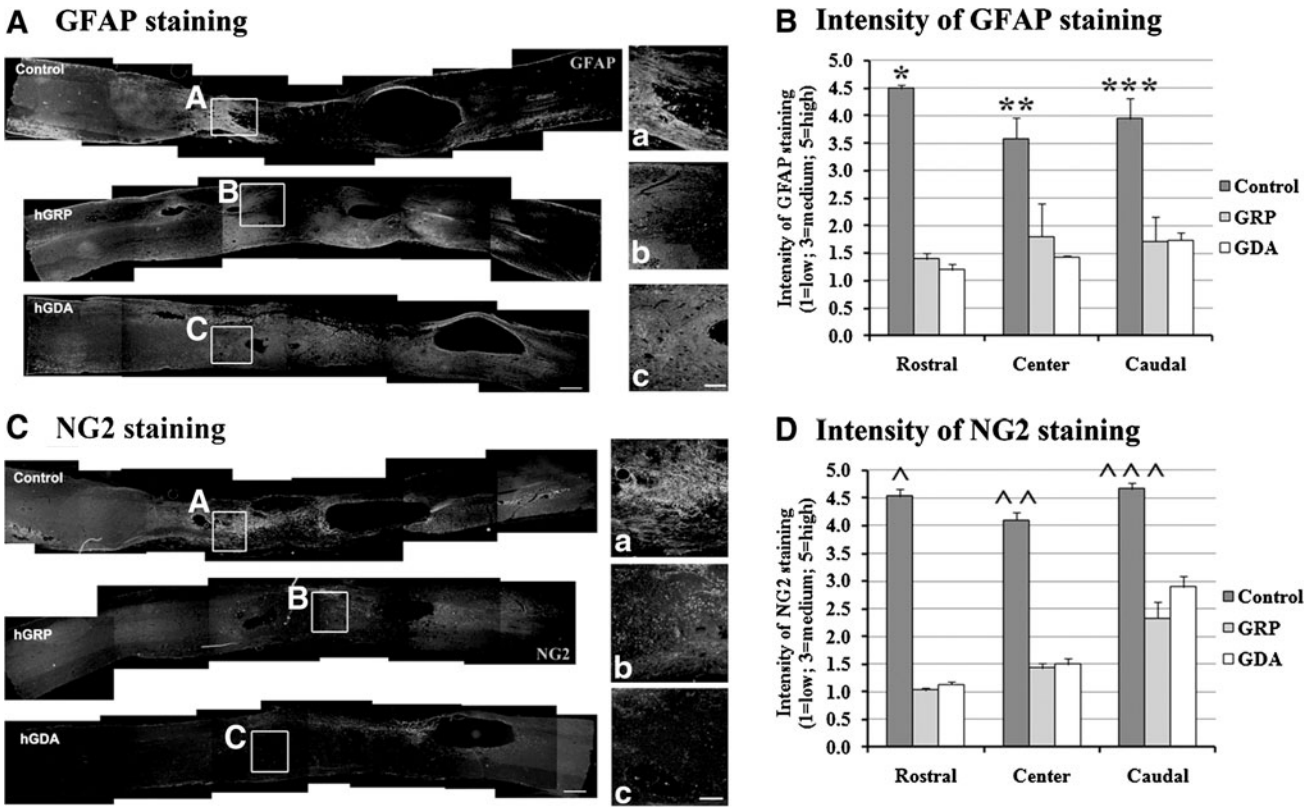

FIG. 4. hGRP and hGDA grafts reduced glial scar formation. (**A**) GFAP staining. In controls, intense GFAP expression indicative of a glial scar was visible surrounding the lesion area. In both transplant groups, GFAP expression was reduced at the host/graft interface (scale bar = 500 μm). Figures **a**, **b**, and **c** represent the areas shown in boxes **A** (control), **B** (hGRP), and **C** (hGDA; scale bar = 200 μm in **a**, **b**, and **c**). (**B**) Intensity of GFAP staining. There was a significant decrease in the intensity of GFAP staining in both the hGRP and hGDA groups compared to the control group in all three areas (in the rostral boundary of the lesion, $*p = 0.000$ for control versus hGRP or hGDA; at the lesion center, $**p = 0.032$ for control versus hGRP, $p = 0.014$ for control versus hGDA; in the caudal boundary of lesion, $***p = 0.008$ for control versus hGRP or hGDA). There was no significant difference between the hGRP and hGDA groups in any area (data are mean ± standard error of the mean [SEM]). (**C**) NG2 staining. Intense NG2 expression was visible surrounding the lesion site in controls. In both transplant groups, NG2 expression was reduced in the host/graft interface (scale bar = 500 μm). Figures **a**, **b**, and **c** represent the areas shown in boxes **A** (control), **B** (hGRP), and **C** (hGDA; scale bar = 200 μm in **a**, **b**, and **c**). (**D**) Intensity of NG2 staining. Intensity of NG2 staining showed a similar pattern to GFAP staining, with significantly reduced intensity of NG2 staining in both the hGRP and hGDA groups compared to the control group (in the rostral boundary of the lesion, $\hat{}p = 0.000$ for control versus hGRP or hGDA; at the lesion center, $\hat{}\hat{}p = 0.000$ for control versus hGRP or hGDA; in the caudal boundary of the lesion, $\hat{}\hat{}\hat{}p = 0.014$ for control versus hGRP, $p = 0.046$ for control versus hGDA). There was no significant difference between the hGRP and hGDA groups in any area (data are mean ± SEM; hGRP, human glial-restricted progenitor; hGDA, astrocytes derived from hGRP; GFAP, glial fibrillary acidic protein).

(data not shown). There was no difference in the distribution of $CGRP^+$ or $5\text{-}HT^+$ axons among the groups.

Plasticity in the lumbar spinal cord

To examine plasticity in the lumbar spinal cord, cross-sections from L6–S1 were stained with CGRP and VR-1 for primary afferent pathways, and with 5-HT for the descending modulatory pathway. We found that both CGRP and VR-1 expression in the dorsal horn of the L6–S1 spinal cord were significantly increased after contusion lesion in all groups compared to sham animals. The results of sprouting of small-diameter dorsal root axons in controls were consistent with previous reports (Krenz and Weaver, 1998, Mitsui et al., 2005). Also, the increase in CGRP-positive fibers was higher, as CGRP-positive fibers (four- to fivefold increases) include small myelinated Aδ-fibers and unmyelinated C-fibers, while VR-1 fibers (threefold increase) represent only unmyelinated C-fibers. The transplants did not have significant effects on the sprouting of CGRP and VR-1 afferent fibers (Fig. 5), but the hGRP group showed a trend toward reduced CGRP sprouting. 5-HT staining in the dorsal horn was decreased after injury; however, hGRP animals expressed significantly higher 5-HT immunoreactivity than the control and hGDA groups, indicating improved connectivity with serotonergic fibers (Fig. 5).

Effects of hGRP and hGDA on recovery of motor, sensory, and bladder functions

Open-field locomotion was assessed using the BBB scale. Before contusion, the rats in all groups were tested to obtain baseline measurements, and the average score for each group was 21. Two to three days after injury, the score had dropped

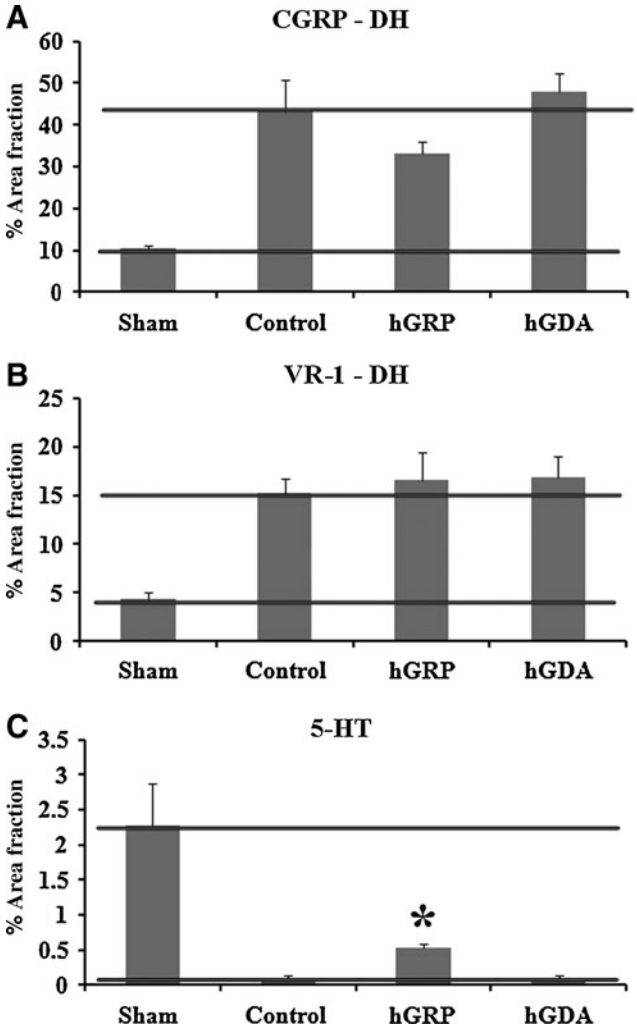

FIG. 5. Quantification by area fraction (%) of immunocytochemical staining in the lumbosacral cord. Shown are (**A**) CGRP, (**B**) VR-1, and (**C**) 5-HT immunoreactivity (IR) in the dorsal horn. For CGRP and VR-1 staining, IR was significantly higher in contused animals compared to sham animals. No significant effect of treatment was observed in hGRP and hGDA animals. 5-HT IR was reduced in all injured animals, but it was significantly higher in hGRP animals than in control or hGDA animals (*$p < 0.05$). The horizontal lines in all panels indicate the levels of sham (uninjured) and injured (untreated) controls. The area between the lines reflects damage to lumbar circuitry after injury (hGRP, human glial-restricted progenitor; hGDA, astrocytes derived from hGRP; CGRP, calcitonin gene-related peptide; 5-HT, serotonin; VR-1, vanilloid receptor type 1).

to 1 in all groups. One week after cell or medium injection, the score increased to 8–9, and then plateaued at 9–10 after 2 weeks, remaining at this score until the end of the experiment in all groups. There were no significant differences among the groups at any tested time point (Supplementary Fig. 3; see online supplementary material at http://www.liebertonline.com).

Grid testing was performed to evaluate sensorimotor function in animals that had recovered BBB scores of at least 10. All animals that could perform the test showed a deficit in

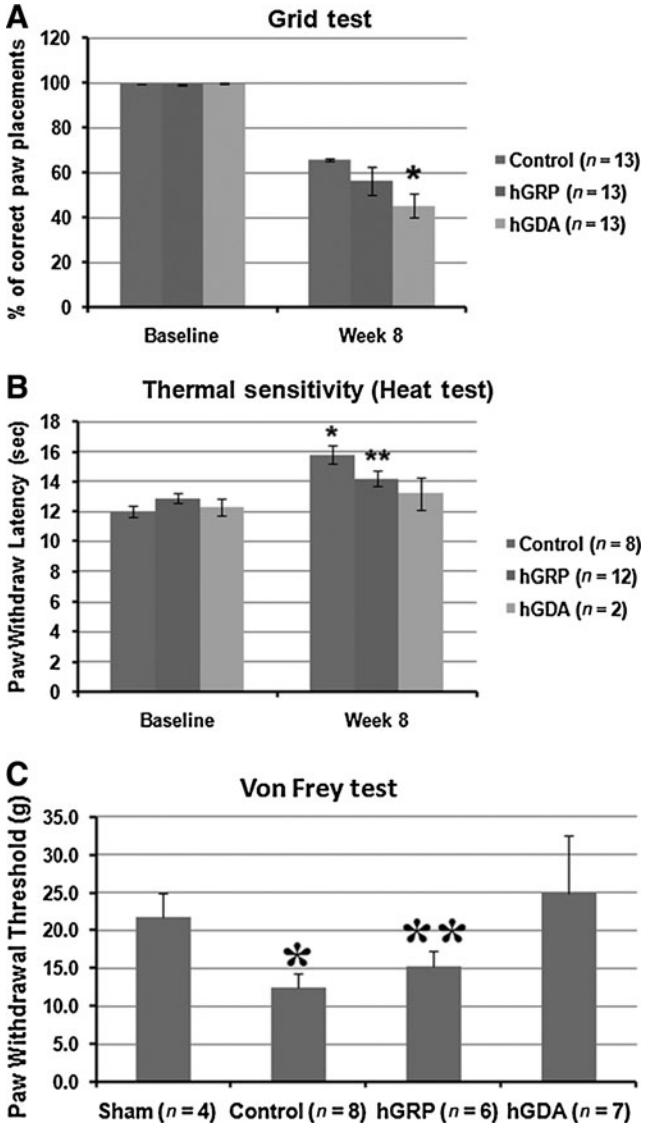

FIG. 6. Recovery of motor-sensory function. (**A**) Results from the grid test showed deficits 8 weeks after transplantation in all groups. A significant reduction in the percentage of correct paw placements was observed in hGDA-transplanted animals compared to controls (*$p < 0.05$). No such difference was observed when we comparing hGRP-transplanted animals to controls. (**B**) Heat testing showed no increase in thermal sensitivity. Rats from the control and hGRP-transplanted groups demonstrated hyposensitivity compared to baseline (**$p < 0.05$ for the hGRP group; *$p < 0.001$ for controls). Results for hGDA-transplanted animals after 8 weeks were not significantly different from baseline; however, the number of rats was small. No significant difference was observed among the experimental groups at 8 weeks. (**C**) Von Frey testing was used to assess mechanical allodynia. Significant differences in paw withdrawal thresholds were observed when sham animals were compared to controls (*$p < 0.01$, $p = 0.002$), and sham animals to hGRP-transplanted animals (**$p < 0.05$, $p = 0.02$) at 8 weeks after transplantation. No significant difference was observed between sham and hGDA-transplanted animals ($p = 0.82$; hGRP, human glial-restricted progenitor; hGDA, astrocytes derived from hGRP).

performance 10 days after injury. By week 8, we observed that animals from the control group performed significantly better than animals from the hGDA group ($p = 0.022$), while animals from the hGRP group were not significantly different from controls (Fig. 6A). Similarly to the grid test, the CatWalk test was performed only on rats that had BBB scores of 10 and above. No more than two rats per group were able to perform on the CatWalk at week 8, making statistically meaningful analysis impossible.

To determine if hGRP or hGDA affected pain perception in transplanted animals, tests for thermal sensitivity (heat test) and mechanical sensitivity (Von Frey test) were performed. The heat test showed significantly increased forepaw withdrawal latency in tested animals in the control ($p < 0.001$) and hGRP ($p < 0.05$) groups at 8 weeks compared to baseline, indicating sensory deficits, but a lack of pain (Fig. 6B). The paw withdrawal threshold in the hGDA group was close to preinjury baseline, suggesting that pain perception had not changed. Von Frey filament testing 8 weeks after transplant showed a significant reduction in paw withdrawal threshold below the level of injury in control animals (Fig. 6C; $p < 0.01$), suggesting an increased sensitivity to tactile stimuli. Treatment with hGRP ($p < 0.05$) did not attenuate this response; however, treatment with hGDA returned paw withdrawal latency to the levels observed prior to injury. Neither of the grafted groups showed decreased latency associated with hypersensitivity or pain.

During regular daily bladder care, bladder size, and urine color were evaluated. By week 8 all animals had clear urine with a small to moderate bladder size. Chemstrip results at that time point were also similar to those observed prior to injury in all animals.

Cystometric data were collected at 8 weeks post-transplantation, prior to sacrifice. Micturition pressures were significantly higher in all contused animals compared to sham animals. No significant differences were observed between the hGRP and hGDA groups compared to controls (Table 2). Rhythmic intravesical pressure waves, indicating DHR, occurred frequently when saline was infused into the bladder in the control and hGDA groups (Fig. 7). These rhythmic contractions were significantly less frequent in the hGRP group ($p < 0.05$), and were almost absent in sham animals, with no difference between the sham and hGRP groups; however, bladder capacity of hGRP-treated rats was significantly higher than that of animals in the other groups, including sham animals. No difference in post-void residual urine was observed in any of the animals. The bladder weight:body weight ratio was significantly higher in all injured animals (control, hGRP, and hGDA) compared to sham animals. Thus the transplants of hGRP appeared to ameliorate DHR, but increased bladder capacity; transplantation of hGDA had no effect on lower urinary tract function.

Discussion

In previous studies rat GRP have been shown to differentiate predominantly into astrocytes, provide neuroprotection, and reduce glial scaring, but not to support significant recovery of function in a contusion model (Cao et al., 2005; Hill et al., 2004; Nout et al., 2010). In contrast, purified populations of immature astrocytes derived from rat GRP (GDA) using BMP treatment have recently been shown to support both anatomical and functional recovery following rubrospinal tract lesion (Davies et al., 2006). We therefore examined the anatomical and functional effects of grafting human glial-restricted progenitors (hGRP), as well as BMP-induced astrocytes (hGDA) in a contusion model of spinal cord injury using athymic rats. In a comprehensive study we have shown for the first time that these human cell populations survived in the injured spinal cord, migrated long distances, differentiated into glial cells, mostly astrocytes, integrated well with the host tissue, and most importantly, reduced CSPG expression and glial scar formation. Despite the anatomical improvement of the lesion environment, neither graft was sufficient to produce significant and broad functional recovery. Nevertheless, the permissive properties of the cells, as well as the lack of sensory hypersensitivity (pain), indicate that hGRP, whose preparation has been designed for clinical use (Sandrock et al., 2010), remain a promising graft for the treatment of SCI.

Graft distribution and phenotype

Cell survival is a critical issue for cell transplantation–based therapies. In this study, hGRP and hGDA were injected into the lesion center as well as rostral and caudal to the lesion 9 days after contusion and survived for 8 weeks. The robust survival of the human cells was facilitated by the use of athymic rats to circumvent the strong immune response associated with xenografts, in accordance with previous studies that also used immune-deficient models (Cummings et al., 2005; Windrem et al., 2004; Yan et al., 2007). Quantitative analysis of total cell numbers indicated modest expansion of the graft with significantly fewer cells observed for hGDA, which were derived from hGRP by a pre-differentiation step with BMP, and were expected therefore to have reduced

Table 2. Urodynamic Parameters by Cystometry and Bladder Weight

Parameter	*Sham* (n = *4*)	*Control* (n = *10*)	*hGRP* (n = *9*)	*hGDA* (n = *6*)
Residual urine (mL)	0 ± 0	0.12 ± 0.08	0.42 ± 0.13	0.13 ± 0.08
Micturition pressure (mm Hg)	15.58 ± 2.58	42.32 ± 4.07*	36.21 ± 1.72*	37.21 ± 2.04*
DHR (no. of episodes/micturition)	0.25 ± 0.15	16.36 ± 5.57*	6.25 ± 0.79#	19.25 ± 1.70*
Bladder capacity (mL)	0.33 ± 0.03	0.60 ± 0.20	1.04 ± 0.10*#	0.53 ± 0.05
Bladder weight:body weight ratio (g)	0.61 ± 0.02	1.3 ± 0.07*	1.43 ± 0.09*	1.38 ± 0.08*

*Significantly different from sham animals, $p < 0.05$.
#Significantly different from control animals, $p < 0.05$.
DHR, detrusor hyperreflexia; hGRP, human glial-restricted progenitor; hGDA, astrocytes derived from hGRP.

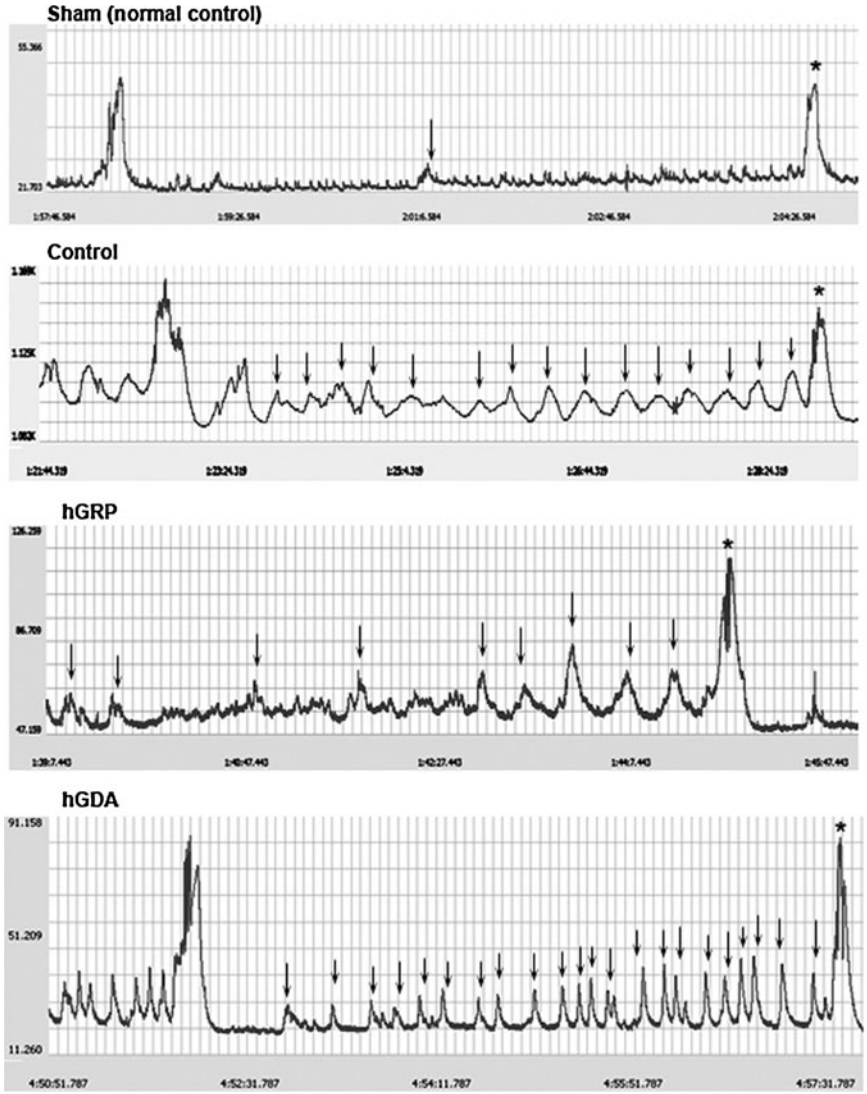

FIG. 7. Representative cystometry readings from the experimental groups. Rhythmic intravesical pressure waves (arrows) were observed before voiding in the control, hGRP, and hGDA groups. These rhythmic contractions were significantly fewer in hGRP-transplanted animals. The micturition pressure (*) was higher in controls than in the hGRP- and hGDA-transplanted animal; however, there were no significant differences among the groups (hGRP, human glial-restricted progenitor; hGDA, astrocytes derived from hGRP).

proliferation (Bonaguidi et al., 2005). Only 3–7% of the cells expressed a mitotic marker (Ki67) at 8 weeks, indicating that most of the proliferation occurred at early stages after transplantation. The limited expansion of the grafts was consistent with similar reports on grafting of human cells in NOD-scid mice (Hooshmand et al., 2009), in which the cells expanded about twofold. This underscores the use of immunodeficient animals as the model of choice for xenograft studies to circumvent extreme immunosuppression protocols and poor graft survival. The grafted cells not only survived near the lesion site, but migrated extensively into host tissue in rostral and caudal directions along white matter tracts. Interestingly, there was a slight bias towards rostral migration, which may reflect preferential injection into the dorsal spinal cord that allowed extensive migration rostrally along the dorsal columns. Cell migration appears to be a common phenomenon for transplanted stem cells in both intact and injured spinal cord (Han et al., 2004; Hill et al., 2004; Hooshmand et al., 2009), making them important vehicles not only for local modification of the host environment, but also for delivery of therapeutic genes distantly (Glaser et al., 2008). We found that 8 weeks after transplantation, hGRP and hGDA differentiated mostly into astrocytes ($GFAP^+$), with a small number of grafted cells at the lesion site differentiating into cells of oligodendrocytic lineage (expressing nuclear $Olig2^+$). While the number of $GFAP^+$ cells decreased along the migration axis from 80% at the lesion epicenter to 40–50% at 6 mm, the number of $Olig2^+$ cells increased dramatically, from $<10\%$ to 40%. These results underscore the strong influence of the host environment upon graft differentiation potential, and suggest that the inflammatory process at the injury site is inhibitory to oligodendrocyte differentiation. The similarities in the expression and distribution of astrocyte and oligodendrocyte markers between hGRP and hGDA grafts stress the influence

of the injury on the phenotypic fate and behavior of glial progenitors, and suggest that the hGDA generated by our predifferentiation protocol (5 days of BMP treatment) could have been attenuated by the injury environment. Our results are consistent with previous studies that examined the challenges of producing oligodendrocytes in the injured spinal cord from either endogenous progenitors or various grafts (McTigue and Tripathi, 2008). These studies concluded that in order to get myelinating oligodendrocytes, it is necessary to use purified populations of oligodendrocyte progenitor cells (OPC; Keirstead et al., 2005; Sharp et al., 2010), or a combination of glial progenitors with specific factors such as neurotrophins (Cao et al., 2005) or ciliary neurotrophic factors, in order to support the myelination process (Cao et al., 2010). It is therefore likely that the Olig2$^+$ cells generated by the grafts represented immature oligodendrocytes. There were almost no graft cells associated with nestin, indicating that at 8 weeks after transplantation, the cells did not remain in an early progenitor state. However, the complexity of the glial progenitor populations in rodents and humans (Liu and Rao, 2004) and the differences in the transplantation protocols and injury models, make direct comparisons of phenotypes difficult, and underscore the importance of characterizing cells, optimizing grafting parameters, and taking into consideration the influence of the injury environment (Bambakidis et al., 2008).

Graft effects on host

In analyzing the effects of the grafted cells on the host, we found that cyst volumes within the transplant area were reduced in the hGRP and hGDA groups compared to cyst volumes in the lesion area, indicating that cells had a beneficial effect, even following delayed transplantation. Similar results suggesting neuroprotective effects after transplantation of rat GRP were recently reported (Nout et al., 2010). Also, transplants of neuronal- and glial-restricted progenitor cells (NRP/GRP) showed increased sparing of host tissue and decreased lesion size (Mitsui et al., 2005), suggesting that at least some of the benefits to the host were derived from GRP. We also found decreased GFAP expression around the lesion area and significant reduction of NG2 expression in both the hGRP and hGDA groups relative to the control injury group, which taken together indicate a dramatic inhibition of scar formation. These results were similar to those of studies of acute transplantation of rat GRP (Hill et al., 2004; Hasegawa et al., 2005), showing a reduced glial scar associated with decreased GFAP expression and CSPG markers. It is interesting to note that the same studies reported large cysts in the transplant site, in contrast to the reduction of cyst volume within the lesion that we observed. It is therefore possible that delayed cell transplantation, which allows better graft survival and is more applicable to clinical translation, is more effective in modulating the lesion cavities than acute transplantation.

Injuries to the CNS activate microglia and macrophages, which accumulate at the lesion site. These inflammatory cells have both beneficial and detrimental effects (Donnelly and Popovich, 2008), and results are therefore difficult to interpret. We found that microglia and macrophages accumulated in the lesion site as well as in adjacent undamaged host tissue in control as well as transplanted groups. It appears that the presence of hGRP and hGDA neither exacerbated nor reduced infiltration of inflammatory cells, which were intermingled with grafted cells, apparently without adverse effects. Similarly, there were no significant changes in microglia/macrophage levels when acute grafts of GRP were analyzed following a contusion injury in which the rats were immunosuppressed with cyclosporin (Hill et al., 2004). Interestingly, a study using a transection lesion in athymic rats (Potas et al., 2006) indicated that in addition to T-cell reduction, macrophage activation is also reduced in athymic rats compared to heterozygous littermates. Given that neither graft elicited a change in microglia and macrophage levels, it is unlikely that the inflammatory response played a major role in the modification of the host environment by grafted cells. This conclusion has to be qualified, however, with respect to immune cells in general, because the use of athymic rats with reduced levels of T cells excluded the full contribution of lymphocytes (Ankeny and Popovich, 2009).

Spinal cord contusion interrupts axons from both ascending and descending tracts, and in the absence of spontaneous regeneration or repair, the results are functional deficits in motor and sensory systems. In the present study, we examined the effects of grafted cells on general axon growth using neurofilament staining, and on regeneration of the afferent axons and descending serotonergic axons. We found that axons were present in spared tissue in all groups, with few axons growing into the lesion site or associated with transplanted cells. No significant differences in axon growth were observed in control versus transplanted groups, suggesting that hGRP and hGDA did not promote axon growth. The failure, particularly of hGDA, to generate a permissive environment for axon growth was surprising, since the rationale for using GRP-induced astrocytes generated by BMP treatment was based on studies that showed that rat GDA grafted into a hemisection injury induced robust axonal regeneration from rubrospinal axons and ascending sensory axons into and out of the lesion, resulting in functional recovery (Davies et al., 2006, 2008). However, a comparison between these studies reveals major differences that include the use of human versus rat cells, a contusion versus hemisection injury model, and delayed versus acute grafting. Indeed, Davies and colleagues cautioned that not all glial precursors will be able to generate beneficial GDA astrocytes by BMP treatments (Davies et al., 2008), and that BMP treatment of acute SCI can promote scar formation (Mabie et al., 1997). In particular it is important to note that most of the published studies utilized rat GRP, while our understanding of the properties of human GRP is limited. As efforts toward the design of clinical trials progress, it becomes critical to elucidate the properties of human cells and to test them *in vivo*. Reports from this and other studies also underscore the challenges of utilizing GRP to effectively modify the host environment as a way to achieve improved function (Hill et al., 2004). It appears therefore that anatomical improvement, which included reducing cysts and suppressing scar formation (as shown in our study and by Hill et al., 2004), were not sufficient to allow significant and broad recovery.

Functional recovery

Although previous studies utilizing neural stem cells have demonstrated functional recovery after SCI, the mechanisms that underlie recovery have not been clearly established, and often the conclusions are based on correlation with

neuroprotection, axonal sprouting, and regeneration or myelination (Bradbury and McMahon, 2006). We have performed a detailed analysis of behavioral tests to examine motor, sensory, and autonomic functions after grafting of hGRP or hGDA. The athymic rats in all experimental groups showed fast functional recovery from the contusion injury in the BBB test, proceeding from a score of 1 at 2–3 days after injury to a score of 8–9 at the end of week 1, reaching a plateau at a score of 10. This profile of rapid recovery in BBB scores following a contusion injury has been observed in other studies of athymic rats, indicating that the athymic phenotype, which is depleted of T cells, affects the recovery process. Nude rats with a transection injury also recovered locomotor function faster than heterozygote and Sprague-Dawley rats (Gorrie et al., 2010; Sheth et al., 2008). Although we found fast recovery in all rats in this experiment, we did not see any differences among groups, indicating that transplants of hGRP or hGDA do not show a beneficial effect on locomotor function. A recent study using rat GRP transplants with or without cAMP and rolipram administration also found no recovery of locomotor function (Nout et al., 2010). Similar results were also found in the grid test. While recovery of function was not significant in either transplanted group compared to controls, rats in the hGDA group showed a modest decrease in correct paw placement.

As previous studies demonstrated that mechanical and thermal allodynia developed in the forelimbs and hindlimbs following contusion injury (Hulsebosch et al., 2000), we examined the effects of our transplants on thermal and mechanical sensitivities using heat and Von Frey test, respectively. The heat test showed that at 8 weeks the control injury and hGRP groups had increased latency of forepaw withdrawal, which indicates a sensory deficit without increased sensitivity to pain. The increased latency seen following injury may be strain-related, since the T-cell deficiency results in a reduced inflammatory response, but is more likely to reflect a body weight and gravity center shift after injury, putting more pressure on the forelimb and causing more contact, which leads to decreased latency. However, the analysis was performed only at 8 weeks before sacrifice, without testing the early response to heat stimulus. The hGDA-transplanted group remained close to the pre-injury baseline, but the number of rats available for testing was too low to have statistical power. In the Von Frey test a significant reduction of the paw withdrawal threshold was found in control injury and hGRP-transplanted rats. In contrast, the hGDA-transplanted animals were no different from uninjured animals, and did not show increased sensitivity to tactile stimuli relative to injured controls. Taken together, these results indicate that even though there was sensory recovery, we did not detect hypersensitivity to pain associated with the grafts in either the mechanical or thermal allodynia tests, which would have been a major concern for clinical application of these cells. Concerns about neuropathic pain have been raised in previous studies that reported increased pain in transplants of neuronal stem cells (Hofstetter et al., 2005) and GRP (Davies et al., 2008); however, other studies with a variety of neural stem cells and progenitors did not find increased pain, and reported improved recovery (Cao et al., 2005, 2010; Cummings et al., 2005; Karimi-Abdolrezaee et al., 2006; Keirstead et al., 2005; Mitsui et al., 2005). Because our grafts included both glial progenitors and astrocytes derived from GRP, and because grafted cells survived and migrated, the lack of pain reported in this study is particularly important in demonstrating that even a large presence of astrocytes at and around the injury site is not necessarily associated with neuropathic pain.

We also examined bladder control as a representative of the effects of hGRP and hGDA on autonomic function following SCI. Bladder dysfunction is caused by damage to descending pathways (e.g., 5-HT), and alterations in primary afferent pathways (e.g., CGRP and VR-1). Urodynamic parameters showed that micturition pressures were high in all injured groups compared to sham animals, but cell transplant groups trended to be lower than the control injury group. Additionally, the occurrence of DHR was reduced in the hGRP group compared to the control and hGDA groups, in a pattern that resembled previous reports of DHR improvement (Mitsui et al., 2003, 2005; Seki et al., 2002). We analyzed CGRP and VR-1 staining to evaluate changes in the small caliber primary afferent pathways to the lumbosacral spinal cord after contusion injury and treatment. The increased CGRP and VR-1 staining observed after the injury in athymic rats was consistent with previous reports in other rat models (Krenz and Weaver, 1998; Mitsui et al., 2005), but the levels of sprouting seen following injury (threefold in VR1 and four- to fivefold in CGRP) may reflect not only the differences in the type of fibers between these tracts, but also the specific response of athymic rats. The improvement we observed in the hGDA group may therefore be related to the small decrease, although not significant, of CGRP staining compared to the hGDA and control groups. In contrast, the increase in 5-HT staining seen in the hGRP versus the hGDA and control groups did not translate into recovery of bladder function, and was not observed in a recent report using rat GRP in a contusion injury, where no differences in the serotonergic input at lumbar levels were found (Nout et al., 2010).

Conclusion

We have demonstrated that hGRP and hGDA grafted into nude rats survived, migrated, and integrated well with host tissue. The grafts improved the lesion environment by reducing cyst volume and glial scar, but these effects were not sufficient to promote axonal growth or produce robust functional recovery. The lack of major differences between hGRP and hGDA indicates similarities between the astrocytes derived from these grafts under the influence of the contusion injury environment. The robust survival and migration of the cells, combined with their beneficial properties with respect to the injury site and the lack of sensory hypersensitivity, indicate that human GRP, which were manufactured for clinical use (Sandrock et al., 2010), and astrocytes, which were derived from GRP, remain a promising graft for the treatment of SCI. Future studies will therefore be focused on improving the injury environment; optimizing transplantation protocols with respect to delay, dose, and differentiation protocols; and may also include interventions that promote axonal growth, such as trophic factors or modified cells.

Acknowledgments

This study was funded by grants from the NIH (P01NS055976), and the CHN Foundation (Linda Kelly, PI). Some of the cells used in this study were manufactured in the Cell Therapy Facility at the University of Utah using Q

Therapeutics technology. We thank Robert Kushner, Carla Tyler-Polsz, and Theresa Connors for technical assistance, and Dr. Mahendra Rao for valuable suggestions.

Author Disclosure Statement

J.T. Campanelli is an employee and shareholder of Q Therapeutics Inc., which is developing cell-based therapeutics to treat degenerative diseases of the CNS. The other authors have no potential conflicts of interest.

References

Ankeny, D.P., and Popovich, P.G. (2009). Mechanisms and implications of adaptive immune responses after traumatic spinal cord injury. Neuroscience 158, 1112–1121.

Bambakidis, N.C., Butler, J., Horn, E.M., Wang, X., Preul, M.C., Theodore, N., Spetzler, R.F., and Sonntag, V.K. (2008). Stem cell biology and its therapeutic applications in the setting of spinal cord injury. Neurosurg. Focus 24, E20.

Basso, D.M., Beattie, M.S., and Bresnahan, J.C. (1995). A sensitive and reliable locomotor rating scale for open field testing in rats. J. Neurotrauma 12, 1–21.

Bonaguidi, M.A., McGuire, T., Hu, M., Kan, L., Samanta, J., and Kessler, J.A. (2005). LIF and BMP signaling generate separate and discrete types of GFAP-expressing cells. Development 132, 5503–5514.

Bradbury, E.J., and McMahon, S.B. (2006). Spinal cord repair strategies: why do they work? Nat. Rev. Neurosci. 7, 644–653.

Cao, Q., He, Q., Wang, Y., Cheng, X., Howard, R.M., Zhang, Y., DeVries, W.H., Shields, C.B., Magnuson, D.S., Xu, X.M., Kim, D.H., and Whittemore, S.R. (2010). Transplantation of ciliary neurotrophic factor-expressing adult oligodendrocyte precursor cells promotes remyelination and functional recovery after spinal cord injury. J. Neurosci. 30, 2989–3001.

Cao, Q., Xu, X.M., Devries, W.H., Enzmann, G.U., Ping, P., Tsoulfas, P., Wood, P.M., Bunge, M.B., and Whittemore, S.R. (2005). Functional recovery in traumatic spinal cord injury after transplantation of multineurotrophin-expressing glial-restricted precursor cells. J. Neurosci. 25, 6947–6957.

Cao, Y., Shumsky, J.S., Sabol, M.A., Kushner, R.A., Strittmatter, S., Hamers, F.P., Lee, D.H., Rabacchi, S.A., and Murray, M. (2008). Nogo-66 receptor antagonist peptide (NEP1-40) administration promotes functional recovery and axonal growth after lateral funiculus injury in the adult rat. Neurorehabil. Neural Repair 22, 262–278.

Chaplan, S.R., Bach, F.W., Pogrel, J.W., Chung, J.M., and Yaksh, T.L. (1994). Quantitative assessment of tactile allodynia in the rat paw. J. Neurosci. Methods 53, 55–63.

Cummings, B.J., Uchida, N., Tamaki, S.J., Salazar, D.L., Hooshmand, M., Summers, R., Gage, F.H., and Anderson, A.J. (2005). Human neural stem cells differentiate and promote locomotor recovery in spinal cord-injured mice. Proc. Natl. Acad. Sci. USA 102, 14069–14074.

Davies, J.E., Huang, C., Proschel, C., Noble, M., Mayer-Proschel, M., and Davies, S.J. (2006). Astrocytes derived from glial-restricted precursors promote spinal cord repair. J. Biol. 5, 7.

Davies, J.E., Proschel, C., Zhang, N., Noble, M., Mayer-Proschel, M., and Davies, S.J. (2008). Transplanted astrocytes derived from BMP- or CNTF-treated glial-restricted precursors have opposite effects on recovery and allodynia after spinal cord injury. J. Biol. 7, 24.

Donnelly, D.J., and Popovich, P.G. (2008). Inflammation and its role in neuroprotection, axonal regeneration and functional recovery after spinal cord injury. Exp. Neurol. 209, 378–388.

Dubois, C., Manuguerra, J.C., Hauttecoeur, B., and Maze, J. (1990). Monoclonal antibody A2B5, which detects cell surface antigens, binds to ganglioside GT3 (II3 (NeuAc)3LacCer) and to its 9-O-acetylated derivative. J. Biol. Chem. 265, 2797–2803.

Glaser, T., Schmandt, T., and Brustle, O. (2008). Generation and potential biomedical applications of embryonic stem cell-derived glial precursors. J. Neurol. Sci. 265, 47–58.

Gorrie, C.A., Hayward, I., Cameron, N., Kailainathan, G., Nandapalan, N., Sutharsan, R., Wang, J., Mackay-Sim, A., and Waite, P.M. (2010). Effects of human OEC-derived cell transplants in rodent spinal cord contusion injury. Brain Res. 1337, 8–20.

Guest, J.D., Rao, A., Olson, L., Bunge, M.B., and Bunge, R.P. (1997). The ability of human Schwann cell grafts to promote regeneration in the transected nude rat spinal cord. Exp. Neurol. 148, 502–522.

Han, S.S., Liu, Y., Tyler-Polsz, C., Rao, M.S., and Fischer, I. (2004). Transplantation of glial-restricted precursor cells into the adult spinal cord: survival, glial-specific differentiation, and preferential migration in white matter. Glia 45, 1–16.

Hasegawa, K., Chang, Y.W., Li, H., Berlin, Y., Ikeda, O., Kane-Goldsmith, N., and Grumet, M. (2005). Embryonic radial glia bridge spinal cord lesions and promote functional recovery following spinal cord injury. Exp. Neurol. 193, 394–410.

Hill, C.E., Proschel, C., Noble, M., Mayer-Proschel, M., Gensel, J.C., Beattie, M.S., and Bresnahan, J.C. (2004). Acute transplantation of glial-restricted precursor cells into spinal cord contusion injuries: survival, differentiation, and effects on lesion environment and axonal regeneration. Exp. Neurol. 190, 289–310.

Himes, B.T., Neuhuber, B., Coleman, C., Kushner, R., Swanger, S.A., Kopen, G.C., Wagner, J., Shumsky, J.S., and Fischer, I. (2006). Recovery of function following grafting of human bone marrow-derived stromal cells into the injured spinal cord. Neurorehabil. Neural Repair 20, 278–296.

Hofstetter, C.P., Holmstrom, N.A., Lilja, J.A., Schweinhardt, P., Hao, J., Spenger, C., Wiesenfeld-Hallin, Z., Kurpad, S.N., Frisen, J., and Olson, L. (2005). Allodynia limits the usefulness of intraspinal neural stem cell grafts; directed differentiation improves outcome. Nat. Neurosci. 8, 346–353.

Hooshmand, M.J., Sontag, C.J., Uchida, N., Tamaki, S., Anderson, A.J., and Cummings, B.J. (2009). Analysis of host-mediated repair mechanisms after human CNS-stem cell transplantation for spinal cord injury: correlation of engraftment with recovery. PLoS One 4, e5871.

Hulsebosch, C.E., Xu, G.Y., Perez-Polo, J.R., Westlund, K.N., Taylor, C.P., and McAdoo, D.J. (2000). Rodent model of chronic central pain after spinal cord contusion injury and effects of gabapentin. J. Neurotrauma 17, 1205–1217.

Jin, Y., Fischer, I., Tessler, A., and Houle, J.D. (2002). Transplants of fibroblasts genetically modified to express BDNF promote axonal regeneration from supraspinal neurons following chronic spinal cord injury. Exp. Neurol. 177, 265–275.

Karimi-Abdolrezaee, S., Eftekharpour, E., Wang, J., Morshead, C.M., and Fehlings, M.G. (2006). Delayed transplantation of adult neural precursor cells promotes remyelination and functional neurological recovery after spinal cord injury. J. Neurosci. 26, 3377–3389.

Keirstead, H.S., Nistor, G., Bernal, G., Totoiu, M., Cloutier, F., Sharp, K., and Steward, O. (2005). Human embryonic stem cell-derived oligodendrocyte progenitor cell transplants remyelinate and restore locomotion after spinal cord injury. J. Neurosci. 25, 4694–4705.

Krenz, N.R., and Weaver, L.C. (1998). Sprouting of primary afferent fibers after spinal cord transection in the rat. Neuroscience 85, 443–458.

Lepore, A.C., Neuhuber, B., Connors, T.M., Han, S.S., Liu, Y., Daniels, M.P., Rao, M.S., and Fischer, I. (2006). Long-term fate of neural precursor cells following transplantation into developing and adult CNS. Neuroscience 142, 287–304.

Liu, Y., and Rao, M.S. (2004). Glial progenitors in the CNS and possible lineage relationships among them. Biol. Cell. 96, 279–290.

Liu, Y., Kim, D., Himes, B.T., Chow, S.Y., Schallert, T., Murray, M., Tessler, A., and Fischer, I. (1999). Transplants of fibroblasts genetically modified to express BDNF promote regeneration of adult rat rubrospinal axons and recovery of forelimb function. J. Neurosci. 19, 4370–4387.

Mabie, P.C., Mehler, M.F., Marmur, R., Papavasiliou, A., Song, Q., and Kessler, J.A. (1997). Bone morphogenetic proteins induce astroglial differentiation of oligodendroglial-astroglial progenitor cells. J. Neurosci. 17, 4112–4120.

McDonald, J.W., Liu, X.Z., Qu, Y., Liu, S., Mickey, S.K., Turetsky, D., Gottlieb, D.I., and Choi, D.W. (1999). Transplanted embryonic stem cells survive, differentiate and promote recovery in injured rat spinal cord. Nat. Med. 5, 1410–1412.

McTigue, D.M., and Tripathi, R.B. (2008). The life, death, and replacement of oligodendrocytes in the adult CNS. J. Neurochem. 107, 1–19.

Mitsui, T., Kakizaki, H., Tanaka, H., Shibata, T., Matsuoka, I., and Koyanagi, T. (2003). Immortalized neural stem cells transplanted into the injured spinal cord promote recovery of voiding function in the rat. J. Urol. 170, 1421–1425.

Mitsui, T., Shumsky, J.S., Lepore, A.C., Murray, M., and Fischer, I. (2005). Transplantation of neuronal and glial restricted precursors into contused spinal cord improves bladder and motor functions, decreases thermal hypersensitivity, and modifies intraspinal circuitry. J. Neurosci. 25, 9624–9636.

Nout, Y.S., Culp, E., Schmidt, M.H., Tovar, C.A., Pröschel, C., Mayer-Pröschel, M., Noble, M.D., Beattie, M.S., and Bresnahan, J.C. (2010). Glial restricted precursor cell transplant with cyclic adenosine monophosphate improved some autonomic functions but resulted in a reduced graft size after spinal cord contusion injury in rats. Exp. Neurol. Doi:10.1016/j.expneurol.2010.10.011.

Potas, J.R., Zheng, Y., Moussa, C., Venn, M., Gorrie, C.A., Deng, C., and Waite, P.M. (2006). Augmented locomotor recovery after spinal cord injury in the athymic nude rat. J. Neurotrauma 23, 660–673.

Raisman, G., and Li, Y. (2007). Repair of neural pathways by olfactory ensheathing cells. Nat. Rev. Neurosci. 8, 312–319.

Ramon-Cueto, A., Plant, G.W., Avila, J., and Bunge, M.B. (1998). Long-distance axonal regeneration in the transected adult rat spinal cord is promoted by olfactory ensheathing glia transplants. J. Neurosci. 18, 3803–3815.

Rao, M.S., Noble, M., and Mayer-Proschel, M. (1998). A tripotential glial precursor cell is present in the developing spinal cord. Proc. Natl. Acad. Sci. USA 95, 3996–4001.

Saito, M., Kitamura, H., and Sugiyama, K. (2001). The specificity of monoclonal antibody A2B5 to c-series gangliosides. J. Neurochem. 78, 64–74.

Sandrock, R.W., Wheatley, W., Levinthal, C., Lawson, J., Hashimoto, B., Rao, M., and Campanelli, J.T. (2010). Isolation, characterization and preclinical development of human glial-restricted progenitor cells for treatment of neurological disorders. Regen. Med. 5, 381–394.

Seki, S., Sasaki, K., Fraser, M.O., Igawa, Y., Nishizawa, O., Chancellor, M.B., de Groat, W.C., and Yoshimura, N. (2002). Immunoneutralization of nerve growth factor in lumbosacral spinal cord reduces bladder hyperreflexia in spinal cord injured rats. J. Urol. 168, 2269–2274.

Sharp, J., Frame, J., Siegenthaler, M., Nistor, G., and Keirstead, H.S. (2010). Human embryonic stem cell-derived oligodendrocyte progenitor cell transplants improve recovery after cervical spinal cord injury. Stem Cells 28, 152–163.

Sheth, R.N., Manzano, G., Li, X., and Levi, A.D. (2008). Transplantation of human bone marrow-derived stromal cells into the contused spinal cord of nude rats. J. Neurosurg. Spine 8, 153–162.

Windrem, M.S., Nunes, M.C., Rashbaum, W.K., Schwartz, T.H., Goodman, R.A., McKhann, G., 2nd, Roy, N.S., and Goldman, S.A. (2004). Fetal and adult human oligodendrocyte progenitor cell isolates myelinate the congenitally dysmyelinated brain. Nat. Med. 10, 93–97.

Xu, X.M., Guenard, V., Kleitman, N., and Bunge, M.B. (1995). Axonal regeneration into Schwann cell-seeded guidance channels grafted into transected adult rat spinal cord. J. Comp. Neurol. 351, 145–160.

Yan, J., Xu, L., Welsh, A.M., Hatfield, G., Hazel, T., Johe, K., and Koliatsos, V.E. (2007). Extensive neuronal differentiation of human neural stem cell grafts in adult rat spinal cord. PLoS Med. 4, e39.

Address correspondence to:
Itzhak Fischer, Ph.D.
Department of Neurobiology and Anatomy
Drexel University College of Medicine
2900 Queen Lane
Philadelphia, PA 19129

E-mail: ifischer@drexelmed.edu